Single molecule detection of DNA-stabilized silver nanoclusters emitting at the NIR I/II border.

Mikkel B. Liisberg,[1] Zahra Shakerikardar,[1] Stacy M. Copp,[2,3] Cecilia Cerretani,[1] Tom Vosch[1,*]

[1] Nanoscience Center and Department of Chemistry, University of Copenhagen, Universitetsparken 5, 2100 Copenhagen, Denmark. Email: tom@chem.ku.dk

[2] Department of Materials Science and Engineering, University of California, Irvine, Irvine, California 92697-2585, United States.

[3] Department of Physics and Astronomy, University of California, Irvine, Irvine, California 92697-4575, United States.

ABSTRACT: The near-infrared (NIR) I and NIR II regions are known for having good light transparency of tissue and less scatter compared to the visible region of the electromagnetic spectrum. However, the number of bright fluorophores in these regions is limited. Here we present a detailed spectroscopic characterization of a DNA-stabilized silver nanocluster (DNA-AgNC) that emits around 960 nm in solution. The DNA-AgNC converts into blue-shifted emitters over time. Embedment of these DNA-AgNCs in polyvinyl alcohol (PVA) show that they are sufficiently bright and photostable to be detected at the single molecule level. Photon antibunching experiments were performed to confirm single emitter behavior. Our findings highlight that screening and exploration of DNA-AgNCs in the NIR II region might yield promising bright and photostable emitters that could help develop bio-imaging applications with unprecedented signal-to-background ratios and single molecule sensitivity.

DNA-stabilized silver nanoclusters (DNA-AgNCs) are a relatively new class of emitters, first introduced in 2004 by Petty *et al.*[11] A large number of DNA sequences have been screened in recent years, yielding DNA-AgNCs covering the visible[22] and the near-infrared (NIR) region.[3, 43, 4] Traditionally, the NIR is divided into two regions, from approximately 650-1000 nm (NIR I) and 1000-1700 nm (NIR II).[5, 65, 6] The NIR II region is sometimes also referred to as the short-wave infrared region (SWIR).[77] While the NIR I region can usually still be covered by standard visible detectors (e.g. multialkali- or silicon-based), venturing into the NIR II region requires a switch of detector material (e.g. InGaAs-based).[88] The NIR I and NIR II regions have gained interest in recent years due to tissue transparency, reduced autofluorescence and reduced light scattering.[5, 7-105, 7-10] Despite these advantageous properties, the number of performant emitters in this spectral region is still limited compared to the visible region.[7, 11-177, 11-17] Several single molecule studies of NIR I emitting DNA-AgNCs have been reported previously in the literature, both immobilized in a polymer matrix and in solution, demonstrating the potential of DNA-AgNCs as suitable NIR I fluorophores.[18-22,18-22] Here we present a detailed photophysical characterization of a DNA-AgNC, approaching the NIR II region (emission maximum 958 nm),[33] which is currently the longest wavelength emitting DNA-AgNC confirmed to be detectable at the single molecule level. Despite being close to the functional edge of silicon detectors,[2323] we demonstrate that this DNA-AgNC can be easily detected at the single molecule level, and some molecules have a sufficient photon flux to perform antibunching experiments, allowing us to confirm single photon emission behavior.[24, 2524,25]

The DNA-AgNC investigated here is stabilized by the DNA-sequence 5'-CGCCCCCACGCGCGGC-3' and a previous study by Swasey *et al.* showed that the emitter is formed by two DNA strands, 12 Ag^0 atoms and 18 Ag^+ cations.[33] As such, it is the largest DNA-stabilized AgNC reported to date. For this DNA-AgNC, an absorption maximum of 854 nm, estimated emission maximum of 953 nm and a fluorescence quantum yield of 7% were reported.[33] The study by Swasey *et al.* was mainly exploratory in nature, presenting a platform for screening and discovery of DNA-AgNCs in the NIR-I region and reporting a number of newly discovered NIR-emissive DNA-AgNCs. Here we studied in detail the photophysical properties and single molecule imaging potential of a specific DNA-AgNC from that study. We synthetized the same DNA-AgNC and details on the synthesis and HPLC-purification (Figures S1 and S5) can be found in the supporting information. Steady-state solution properties of the

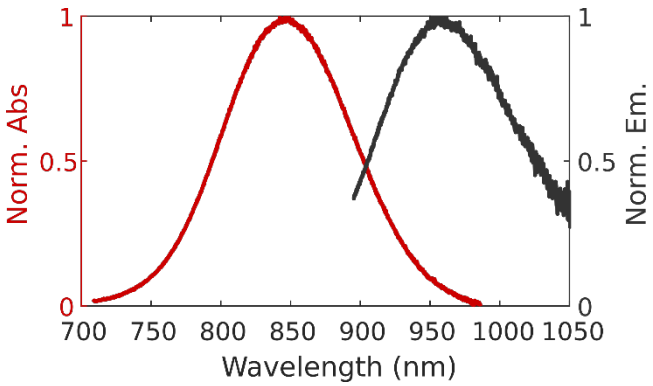

Figure 1. Normalized absorption and emission spectra of a DNA-AgNC solution droplet with 10 mM ammonium acetate (NH_4OAc) measured on top of a confocal microscope. The emission spectrum was recorded by exciting at 850 nm. All data are for the fraction collected at 14.4 – 15.3 minutes in Figure S1

DNA-AgNC were investigated by placing a droplet of the HPLC-purified DNA-AgNC solution on a home-built single molecule sensitive confocal microscope.[2626] The normalized absorption and emission spectra can be found in Figure 1 (see Figure S2 for details on axes calibration). The obtained absorption and emission maxima of 848 nm and 958 nm are in good agreement with the values by Swasey *et al.*[33]

To assess the number of distinct emitters in the collected fraction, emission spectra were recorded by varying the excitation wavelength from 690 to 890 nm (Figure 2A and Figure S3). We observe a shift of emission maximum with excitation wavelength and a secondary blue-shifted peak at ~800 nm for 700 nm excitation (Figure 2B). Such behavior has been observed for unpurified solutions containing multiple spectrally different emitters.[1, 271, 27] While the sample that we study here is HPLC-purified, it is very likely that more than one distinct emitter was collected in the 14.4 – 15.3 minutes range (minimum two emitters, one with a maximum around 800 nm and one around 958 nm). Changing excitation wavelengths from 890 to 730 nm caused the overall emission maxima to blue-shift, indicating the presence and more preferential excitation of blue-shifted emitters. Below 730 nm, the overall emission maximum starts to shift back to 958 nm (Figure 2B), most likely due to preferential excitation into a higher excited state of the 958 nm emitter. Figure S4 supports this hypothesis, showing that for 690 nm and 890 nm excitation, the shape and maxima of the 958 nm emission peak overlap well.

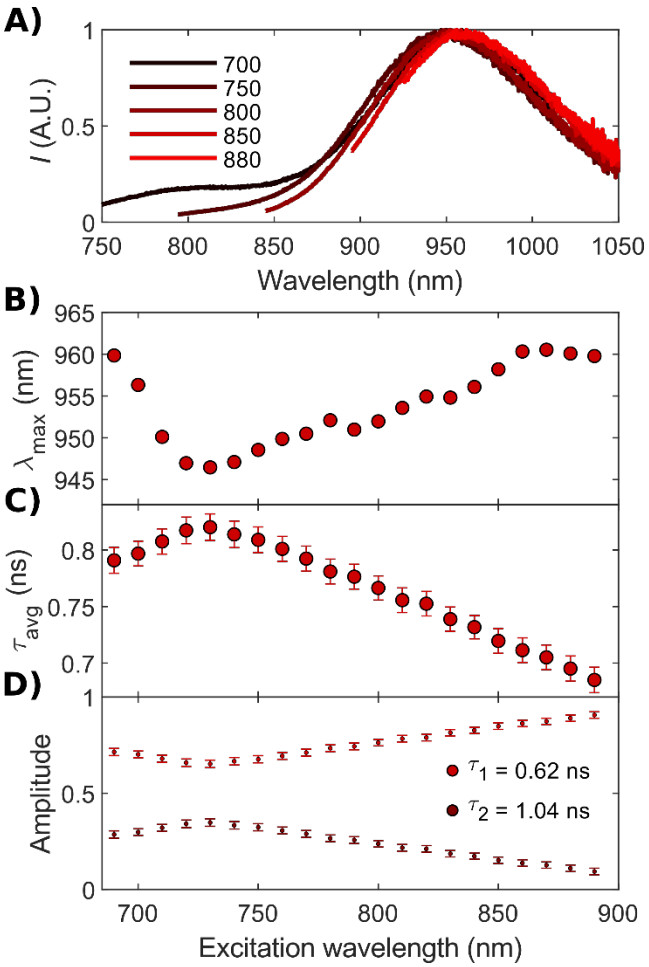

Figure 2. A) Normalized emission spectra, excited at different wave-lengths of a 10 mM NH_4OAc containing DNA-AgNC solution droplet measured on top of a confocal microscope. B) Emission maxima from exciting in the 690 nm to 890 nm range. C) Intensity weighted average decay times (τ_{avg}) at different excitation wavelengths and D) normalized amplitudes of the global fitted bi-exponential decay curves in the excitation range from 690 nm to 890 nm. Decay curves and an example of a fit can be found in Figure S9 and S10. All data are taken for the 14.4 – 15.3 minutes fraction in Figure S1.

The hypothesis that more than one distinct emitter was collected in the HPLC fraction was confirmed by increasing the collection range from 13 – 16 minutes (see Figures S5, S6 and S7), which showed an even more continuous shifting of the emission spectrum with changing excitation wavelength. The overall trend in the shift of the emission maxima with excitation wavelength is more gradual (less bimodal as compared to Figure 2), indicating that a larger range of spectrally similar species are collected in the 13 – 16 minutes fraction. While one could potentially further optimize the HPLC-purification to collect solely the 958 nm emitter, Figure S8 shows that exposure of a freshly collected fraction to ambient conditions, broadens the absorption spectrum and produces an additional shoulder around 750 nm (see Figure S4). This indicates that even if a pure 958 nm emitter is collected, this pure product is likely to evolve into spectrally blue-shifted emitters over time. The exact nature of this spectral conversion/broadening over time is not currently understood, and we do not pursue further HPLC purification efforts here. Previously, oxidation/reduction and conformational changes have been identified for other DNA-AgNCs to cause spectral conversion.[28, 2928,29]

Time-correlated single photon counting (TCSPC) also confirmed the presence of more than one distinct emitter. The purest fraction obtained (14.4 – 15.3 minutes fraction in Figure S1) required fitting of the decay curves with a bi-exponential function. The bi-exponential fit does not necessarily mean that only two emitters are present, but only that two decay components can satisfactorily fit the decay curve of the emitters present in solution. The change of the intensity averaged decay time (τ_{avg}) as a function of excitation wavelength can be found in Figure 2C. Decay components of 0.62 ns and 1.04 ns were obtained from the bi-exponential global fit,[3030] and the normalized amplitude of each decay component can be seen in Figure 2D. The wavelength-dependent evolution of the amplitude of the 0.62 ns component correlates well with the dominant 958 nm emitter in the collected fraction, indicating that this is the decay time of the 958 nm emitter (Figure 2C).

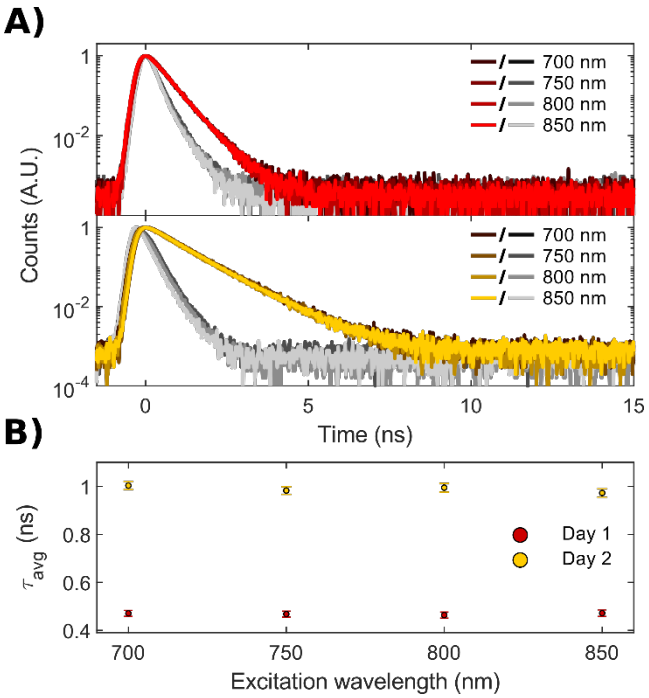

Figure 3. Decay curves of DNA-AgNCs in PVA excited at 700, 750, 800, and 850 nm. A) Decay curves (colored traces) and IRFs (grey traces) recorded immediately after preparation of the spin-coated sample (top panel), and after leaving the sample overnight exposed to ambient conditions (lower panel). B) Intensity averaged decay times (bi-exponential tail-fit) of the sample by measuring immediately after spin-coating (Day 1) and overnight exposed to ambient conditions (Day 2). Data from the purified fraction that was collected around 14.4 – 15.3 minutes in Figure S1.

While the collected fraction contains more than one distinct emitter, and can evolve over time, the main purpose of this study is to investigate whether the DNA-AgNCs were bright and photostable enough to be detected at the single molecule level. Since we plan to investigate the single molecule immobilized in polyvinyl alcohol (PVA), we first studied the ensemble properties of the DNA-AgNCs mixed with a PVA solution and spincoated on a cleaned glass coverslip. Similar steady-state and time-resolved fluorescence measurements were performed in PVA to compare the properties of the DNA-AgNCs in PVA versus the 10 mM NH_4OAc solution. Figure 3 and Figure S11 show that the behavior of the DNA-AgNCs embedded in PVA was similar to the DNA-AgNC in solution. For freshly spincoated DNA-AgNC in PVA, excitation at 850 nm produces an emission maximum at 955 nm (Figure S11), as compared to 958 nm in solution (Figure 2B). The τ_{avg} value was 0.47 ns in PVA (Figure 3B), a bit shorter than the solution τ_{avg} value of 0.72 ns (Figure 2C). When the same DNA-AgNC PVA film was measured the next day, excitation at 850 nm produced an emission maximum at 917 nm (Figure S11) and a τ_{avg} value of 0.95 ns (Figure 3B). This blue-shift is similar to the behavior of the solution sample (Figure S8), indicating that exposure to ambient conditions seems to enhance the contribution of the blue-shifted emitters in PVA, as well. The increase of τ_{avg} to 0.95 ns also agrees with the increasing weight of the 1.04 ns decay component for blue-shifted emitters in solution (Figure 2C).

Next, the DNA-AgNC solution was further diluted to concentrations that yielded individual spots when mixed with PVA, and spin-coated on a cleaned glass coverslip. Figures 4A show a typical example of such a confocal microscopy image (see SI for more examples). The decay times determined from the single spots follow the bulk PVA trend. On day 1, 154 spots showed a bimodal distribution of decay times centered around 0.57 and 0.80 ns, while 168 spots measured on day 2 showed a distribution of decay times centered around 1.02 ns (see Figure 4B). Due to the limited signal of the individual molecules, we did not simultaneously measure the emission spectrum. However, the similar trend of the decay times from the single spots over time support that the spectra of the single spots on day 2 also likely blue-shifted with respect to the original 958 nm emitter, confirming that the single molecule behavior is in line with the ensemble PVA results.

We next split the available fluorescence photons onto two detectors to construct photon antibunching histograms, probing whether these spots are indeed single DNA-AgNC molecules or aggregates.[24, 3124, 31] While the signal from the 322 spots was more than sufficient to construct fluorescence time trajectories and decay curves, the photon flux requirements to create an antibunching histogram are more demanding. Only 41 spots were bright and photostable enough to construct a photon antibunching histogram that yielded N_C/N_L ratios (N_C: counts of the central peak at zero delay, N_L: the average counts of the 10 lateral peaks) below 0.5.[2424]

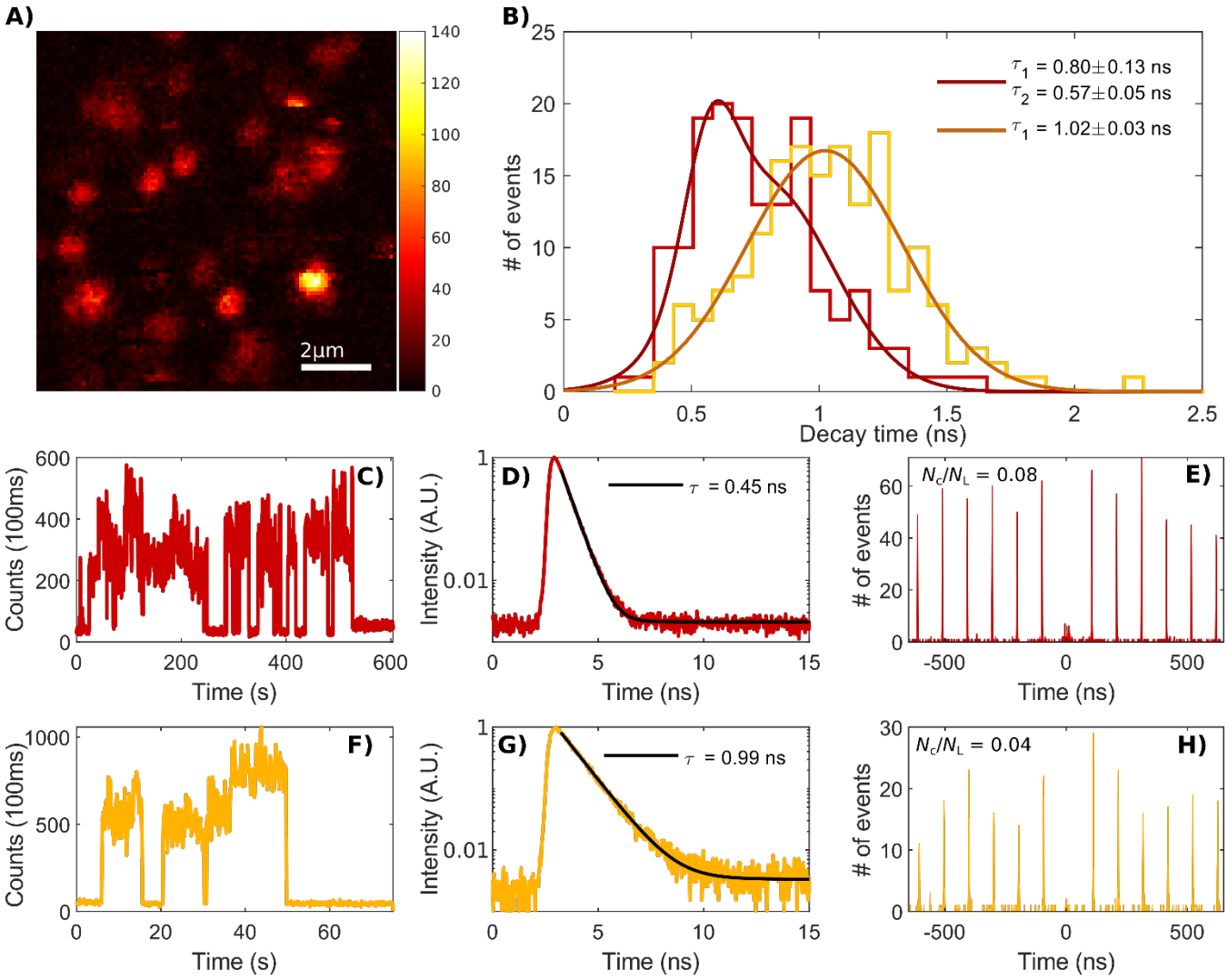

Figure 4. A) Scanning confocal image of the DNA-AgNCs embedded in PVA. B) Histograms of decay times obtained from tail-fitting decay curves of single spots with a mono-exponential fit. Histograms of decay times measured on the same (day 1, 154 entries) and following (day 2, 168 entries) day of sample preparation are shown in red and yellow, respectively. The histogram from day 1 shows a bimodal distribution that was fitted with two Gaussian functions. The short-lived population is depleted by leaving it overnight and can ultimately be fitted with a single Gaussian on day 2. Errors on the center of the Gaussians are given as the 95% confidence intervals. C) Fluorescence intensity trajectory from a single molecule measured on the day of preparation. D) Corresponding normalized decay curve and decay time, calculated by tail-fitting a mono-exponential function to the data, of the same molecule in C). E) Antibunching histogram of the molecule shown in C). For display purposes the actual delay of 1.64 µs between the two detectors was subtracted from the x-axis values. F-H) Similar as for C-E) but now for a molecule measured the day after sample preparation.

Figures 4C-E and 4F-H show respective examples from day 1 and day 2. For these two particular molecules, τ_{avg} values of 0.45 and 0.99 ns and N_C/N_L ratios of 0.08 and 0.04 were found. Five additional examples from day 1 and day 2 can be found in the SI. Due to the limited number of photons in the individual histograms (see for example Figure 4E and 4H), combined photon antibunching histograms were constructed and can be found in Figures S12 and S13, demonstrating that the majority of spots showed clear single photon emitter behavior. Even though it has been demonstrated that Förster resonance energy transfer (FRET) processes are able to make multichromophoric systems behave as single photon emitters, due to FRET-based annihilation processes (e.g. singlet-singlet annihilation),[25, 31, 3225, 31, 32] we are confident that most of the examples provided here and in the SI are observations of single DNA-AgNC molecules. Reasons for this (besides the low N_C/N_L ratio) are the dilute nature of the DNA-AgNC solution, the single exponential decay times of the isolated spots monitored in the PVA film, the single-step blinking and photobleaching behavior. Additionally, a clear DNA-AgNC aggregate example is provided in section 9.1 of the SI. The aggregate example shows a gradual, almost exponential-like decrease in fluorescence intensity, a N_C/N_L ratio of 0.86 and a fluorescence decay curve that is clearly multi-exponential.

In conclusion, our results show that the particular DNA-AgNC 958 nm emitter studied here displays some intriguing conversion dynamics and spectral broadening over time, both in solution and PVA film. It is promising that both the initial 958 nm emitter (predominantly present on day one in the PVA) and the blue-shifted conversion products can be

detected with single molecule sensitivity at the NIR I/II border. This is despite the technical limitation of the equipment used, which diminished the potential achievable signal: at the NIR I/II border, the avalanche photodiodes have limited photon detection efficiencies, and the optical coatings in the microscope were designed for the visible wavelength range. Our findings should encourage further exploration and discovery of more stable, non-converting DNA-AgNCs in the NIR I region and especially the NIR II region.[3333] Together with equipment more suitable for NIR detection and verification that similar performance is achieved in relevant media (biological media[3434] instead of a PVA polymer film), DNA-AgNCs could become relevant emitters for enabling single molecule fluorescence applications in the NIR II region.

ASSOCIATED CONTENT

Supporting Information. Material and methods section, HPLC chromatograms, calibration information, additional absorption and emission spectra, fluorescence decay curves, additional single molecule data and confocal images. This material is available free of charge via the Internet at http://pubs.acs.org.

AUTHOR INFORMATION

Corresponding Author

* E-mail: tom@chem.ku.dk

Notes

The authors declare no competing financial interest.

ACKNOWLEDGMENT

M.B.L., C.C and T.V. acknowledge funding from the Villum Foundation (VKR023115) and the Independent Research Fund Denmark (0136-00024B). We thank Peter Dedecker for providing the antibunching analysis routine. Z.S. acknowledges financial support from the Erasmus + Program. S.M.C acknowledges funding from NSF-CBET- 2025790.

REFERENCES

1. Petty, J. T.; Zheng, J.; Hud, N. V.; Dickson, R. M., DNA-Templated Ag Nanocluster Formation. Journal of the American Chemical Society 2004, 126 (16), 5207-5212.

2. Copp, S. M.; Gorovits, A.; Swasey, S. M.; Gudibandi, S.; Bogdanov, P.; Gwinn, E. G., Fluorescence color by data-driven design of genomic silver clusters. ACS Nano 2018, 12 (8), 8240-8247.

3. Swasey, S. M.; Copp, S. M.; Nicholson, H. C.; Gorovits, A.; Bogdanov, P.; Gwinn, E. G., High throughput near infrared screening discovers DNA-templated silver clusters with peak fluorescence beyond 950 nm. Nanoscale 2018, 10 (42), 19701-19705.

4. Swasey, S. M.; Nicholson, H. C.; Copp, S. M.; Bogdanov, P.; Gorovits, A.; Gwinn, E. G., Adaptation of a visible wavelength fluorescence microplate reader for discovery of near-infrared fluorescent probes. Review of Scientific Instruments 2018, 89 (9), 095111.

5. Zhu, S.; Tian, R.; Antaris, A. L.; Chen, X.; Dai, H., Near-Infrared-II Molecular Dyes for Cancer Imaging and Surgery. Advanced Materials 2019, 31 (24), 1900321.

6. East, A. K.; Lucero, M. Y.; Chan, J., New directions of activity-based sensing for in vivo NIR imaging. Chemical Science 2020.

7. Cosco, E. D.; Spearman, A. L.; Ramakrishnan, S.; Lingg, J. G. P.; Saccomano, M.; Pengshung, M.; Arús, B. A.; Wong, K. C. Y.; Glasl, S.; Ntziachristos, V.; Warmer, M.; McLaughlin, R. R.; Bruns, O. T.; Sletten, E. M., Shortwave infrared polymethine fluorophores matched to excitation lasers enable non-invasive, multicolour in vivo imaging in real time. Nature Chemistry 2020.

8. Cao, J.; Zhu, B.; Zheng, K.; He, S.; Meng, L.; Song, J.; Yang, H., Recent Progress in NIR-II Contrast Agent for Biological Imaging. Frontiers in Bioengineering and Biotechnology 2020, 7 (487).

9. Pansare, V. J.; Hejazi, S.; Faenza, W. J.; Prud'homme, R. K., Review of Long-Wavelength Optical and NIR Imaging Materials: Contrast Agents, Fluorophores, and Multifunctional Nano Carriers. Chemistry of Materials 2012, 24 (5), 812-827.

10. Hong, G.; Diao, S.; Chang, J.; Antaris, A. L.; Chen, C.; Zhang, B.; Zhao, S.; Atochin, D. N.; Huang, P. L.; Andreasson, K. I.; Kuo, C. J.; Dai, H., Through-skull fluorescence imaging of the brain in a new near-infrared window. Nature Photonics 2014, 8 (9), 723-730.

11. Endo, T.; Ishi-Hayase, J.; Maki, H., Photon antibunching in single-walled carbon nanotubes at telecommunication wavelengths and room temperature. Applied Physics Letters 2015, 106 (11), 113106.

12. Fuchs, F.; Stender, B.; Trupke, M.; Simin, D.; Pflaum, J.; Dyakonov, V.; Astakhov, G. V., Engineering near-infrared single-photon emitters with optically active spins in ultrapure silicon carbide. Nature Communications 2015, 6 (1), 7578.

13. Fu, M.; Tamarat, P.; Trebbia, J.-B.; Bodnarchuk, M. I.; Kovalenko, M. V.; Even, J.; Lounis, B., Unraveling exciton–phonon coupling in individual FAPbI3 nanocrystals emitting near-infrared single photons. Nature Communications 2018, 9 (1), 3318.

14. Deutsch, Z.; Schwartz, O.; Tenne, R.; Popovitz-Biro, R.; Oron, D., Two-Color Antibunching from Band-Gap Engineered Colloidal Semiconductor Nanocrystals. Nano Letters 2012, 12 (6), 2948-2952.

15. He, X.; Hartmann, N. F.; Ma, X.; Kim, Y.; Ihly, R.; Blackburn, J. L.; Gao, W.; Kono, J.; Yomogida, Y.; Hirano, A.; Tanaka, T.; Kataura, H.; Htoon, H.; Doorn, S. K., Tunable room-temperature single-photon emission at telecom wavelengths from sp3 defects in carbon nanotubes. Nature Photonics 2017, 11 (9), 577-582.

16. Li, Q.; Zhou, D.; Chai, J.; So, W. Y.; Cai, T.; Li, M.; Peteanu, L. A.; Chen, O.; Cotlet, M.; Wendy Gu, X.; Zhu, H.; Jin, R., Structural distortion and electron redistribution in dual-emitting gold nanoclusters. Nature Communications 2020, 11 (1), 2897.

17. Lange, L.; Schäfer, F.; Biewald, A.; Ciesielski, R.; Hartschuh, A., Controlling photon antibunching from 1D emitters using optical antennas. Nanoscale 2019, 11 (31), 14907-14911.

18. Vosch, T.; Antoku, Y.; Hsiang, J. C.; Richards, C. I.; Gonzalez, J. I.; Dickson, R. M., Strongly emissive individual DNA-encapsulated Ag nanoclusters as single-molecule fluorophores. Proceedings of the National Academy of Sciences of the United States of America 2007, 104 (31), 12616-12621.

19. Hooley, E. N.; Paolucci, V.; Liao, Z.; Carro Temboury, M. R.; Vosch, T., Single-Molecule Characterization of Near-Infrared-Emitting Silver Nanoclusters. Advanced Optical Materials 2015, 3 (8), 1109-1115.

20. Petty, J. T.; Fan, C.; Story, S. P.; Sengupta, B.; St. John Iyer, A.; Prudowsky, Z.; Dickson, R. M., DNA encapsulation of 10 silver atoms producing a bright, modulatable, near-infrared-emitting cluster. Journal of Physical Chemistry Letters 2010, 1 (17), 2524-2529.

21. Petty, J. T.; Fan, C.; Story, S. P.; Sengupta, B.; Sartin, M.; Hsiang, J. C.; Perry, J. W.; Dickson, R. M., Optically enhanced, near-IR, silver cluster emission altered by single base changes in the DNA template. Journal of Physical Chemistry B 2011, 115 (24), 7996-8003.

22. Sharma, J.; Yeh, H.-C.; Yoo, H.; Werner, J. H.; Martinez, J. S., A complementary palette of fluorescent silver nanoclusters. Chemical Communications 2010, 46 (19), 3280-3282.

23. Van den Eynde, R.; Sandmeyer, A.; Vandenberg, W.; Duwé, S.; Hübner, W.; Huser, T.; Dedecker, P.; Müller, M., Quantitative comparison of camera technologies for cost-effective super-resolution optical fluctuation imaging (SOFI). Journal of Physics: Photonics 2019, 1 (4), 044001.

24. Weston, K. D.; Dyck, M.; Tinnefeld, P.; Müller, C.; Herten, D. P.; Sauer, M., Measuring the Number of Independent Emitters in Single-Molecule Fluorescence Images and Trajectories Using Coincident Photons. Analytical Chemistry 2002, 74 (20), 5342-5349.
25. Tinnefeld, P.; Weston, K. D.; Vosch, T.; Cotlet, M.; Weil, T.; Hofkens, J.; Müllen, K.; De Schryver, F. C.; Sauer, M., Antibunching in the Emission of a Single Tetrachromophoric Dendritic System. Journal of the American Chemical Society 2002, 124 (48), 14310-14311.
26. Liao, Z.; Hooley, E. N.; Chen, L.; Stappert, S.; Müllen, K.; Vosch, T., Green Emitting Photoproducts from Terrylene Diimide after Red Illumination. Journal of the American Chemical Society 2013, 135 (51), 19180-19185.
27. Carro Temboury, M. R.; Paolucci, V.; Hooley, E. N.; Latterini, L.; Vosch, T., Probing DNA-stabilized fluorescent silver nanocluster spectral heterogeneity by time-correlated single photon counting. Analyst 2016, 141 (1), 123-130.
28. Cerretani, C.; Vosch, T., Switchable Dual-Emissive DNA-Stabilized Silver Nanoclusters. ACS Omega 2019, 4 (4), 7895-7902.
29. Petty, J. T.; Sergev, O. O.; Nicholson, D. A.; Goodwin, P. M.; Giri, B.; McMullan, D. R., A Silver Cluster–DNA Equilibrium. Analytical Chemistry 2013, 85 (20), 9868-9876.
30. Janssens, L. D.; Boens, N.; Ameloot, M.; De Schryver, F. C., A systematic study of the global analysis of multiexponential fluorescence decay surfaces using reference convolution. The Journal of Physical Chemistry 1990, 94 (9), 3564-3576.
31. Masuo, S.; Vosch, T.; Cotlet, M.; Tinnefeld, P.; Habuchi, S.; Bell, T. D. M.; Oesterling, I.; Beljonne, D.; Champagne, B.; Müllen, K.; Sauer, M.; Hofkens, J.; De Schryver, F. C., Multichromophoric Dendrimers as Single-Photon Sources: A Single-Molecule Study. The Journal of Physical Chemistry B 2004, 108 (43), 16686-16696.
32. Schedlbauer, J.; Wilhelm, P.; Grabenhorst, L.; Federl, M. E.; Lalkens, B.; Hinderer, F.; Scherf, U.; Höger, S.; Tinnefeld, P.; Bange, S.; Vogelsang, J.; Lupton, J. M., Ultrafast Single-Molecule Fluorescence Measured by Femtosecond Double-Pulse Excitation Photon Antibunching. Nano Letters 2020, 20 (2), 1074-1079.
33. Neacşu, V. A.; Cerretani, C.; Liisberg, M. B.; Swasey, S. M.; Gwinn, E. G.; Copp, S. M.; Vosch, T., Unusually large fluorescence quantum yield for a near-infrared emitting DNA-stabilized silver nanocluster. Chemical Communications 2020, 56 (47), 6384-6387.
34. Choi, S.; Dickson, R. M.; Yu, J., Developing luminescent silver nanodots for biological applications. Chemical Society Reviews 2012, 41 (5), 1867-1891.

SYNOPSIS TOC